

000  
001  
002  
003 

# BATCH SPECULATIVE DECODING DONE RIGHT

  
004  
005  
006  
007  
008  
009  
010  
011  
012  
013  
014  
015  
016  
017  
018  
019  
020  
021  
022  
023  
024  
025  
026  
027

**Anonymous authors**

Paper under double-blind review

## ABSTRACT

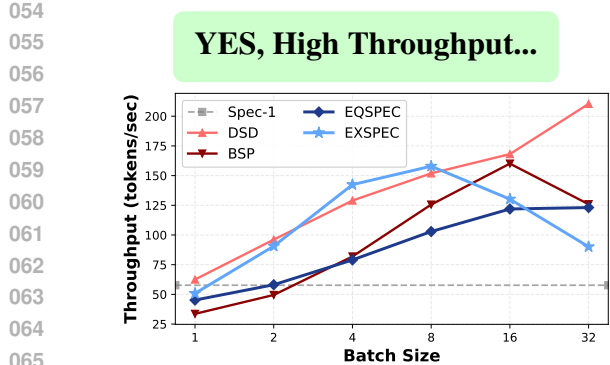
Speculative decoding speeds up LLM inference by using a small draft model to propose multiple tokens that a target model verifies in parallel. Extending this idea to batches is essential for production serving, but it introduces the ragged tensor problem: sequences in the same batch accept different numbers of draft tokens, breaking right-alignment and corrupting position IDs, attention masks, and KV-cache state. We show that several existing batch implementations violate output equivalence—the fundamental requirement that speculative decoding must produce identical token sequences to standard autoregressive generation. These violations occur precisely due to improper handling of the ragged tensor problem. In response, we (1) characterize the synchronization requirements that guarantee correctness, (2) present a correctness-first batch speculative decoding EQSPEC that exposes realignment as consuming 40% of overhead, and (3) introduce EXSPEC, which maintains a sliding pool of sequences and dynamically forms same-length groups, to reduce the realignment overhead while preserving per-sequence speculative speedups. On the SpecBench dataset, across Vicuna-7B/68M, Qwen3-8B/0.6B, and GLM-4-9B/0.6B target/draft pairs, our approach achieves up to 3 $\times$  throughput improvement at batch size 8 compared to batch size 1, with efficient scaling through batch size 8, while maintaining 95% output equivalence. Our method requires no custom kernels and integrates cleanly with existing inference stacks.

## 1 INTRODUCTION

Speculative decoding (Leviathan et al., 2023; Chen et al., 2023) accelerates LLM inference by using a small draft model to propose multiple tokens that the target model verifies in parallel, shifting from memory-bound sequential generation to compute-intensive verification and delivering single-sequence speedups (Xia et al., 2024). Batch speculative decoding aims to combine this per-sequence acceleration with standard batching by processing multiple sequences (batch dimension) while verifying multiple draft tokens per sequence (sequence dimension). The core challenge is the ragged-tensor effect (Qian et al., 2024): in each verification round, sequences accept a single series of the proposed draft tokens, but prefix lengths differ across sequences (e.g., one accepts five tokens while another accepts one), misaligning sequence lengths. This raggedness violates the rectangular-tensor assumption required for GPU-parallel execution.

Figure 1 highlights a critical, often overlooked issue in batch speculative decoding: methods with impressive throughput can produce **corrupted** outputs. For lossless acceleration, speculative decoding must yield **identical** outputs to standard autoregressive generation (Leviathan et al., 2023). As a reference point, the widely used HuggingFace implementation (Wolf et al., 2020) preserves this guarantee, but only for batch size 1. By contrast, in our tests of public batch implementations—specifically, BSP (Su et al., 2023) and DSD (Yan et al., 2025)—this requirement is violated at batch sizes  $> 1$ , manifesting as repetitive tokens or <unk> symbols under greedy decoding rather than matching standard generation.

These failures share a single root cause—broken synchronization invariants (position tracking, attention, KV-cache) across ragged tensors. We first propose EQSPEC by formalizing these invariants and enforcing them with synchronization-aware scheduling (Section 3.1). Concretely, EQSPEC specifies the minimal synchronization needed for correctness and shows that realignment accounts for 40% of computation—an inherent cost of maintaining invariants across ragged tensors. This fundamental overhead helps explain why even production systems struggle: vLLM’s speculative decoding under-



→ BUT, Output Gibberish!

Method	Generated Output
<i>Prompt: "The weather today is"</i>	
Ground Truth	not as bad as it was yesterday...
Spec-1	✓ Matches ground truth
BSP	✗ not not not not not not...
DSD	✗ (unk) (unk) The perfect time...
EQSPEC	✓ Matches ground truth
EXSPEC	✓ Matches ground truth

066  
067  
068  
069  
Figure 1: Batch speculative decoding on Vicuna-7B/68M: Existing methods achieve high throughput but **violate the fundamental requirement of output equivalence** by producing corrupted outputs. Our approach maintains perfect correctness while still achieving competitive performance.

070  
071  
072  
073  
performs its non-speculative baseline at higher batch sizes (leading to deprecation in its v1 engine), while SGLang with EAGLE (Li et al., 2024a) consistently exhibits negative speedups. Our analysis indicates that the superlinear growth of synchronization overhead is an inevitable cost of correctness in batch speculative decoding—a barrier no existing system has overcome.

074  
075  
076  
077  
078  
079  
080  
081  
To address this in practice, our main algorithm EXSPEC (Section 3.3) expands the scheduling scope: it maintains a sliding window of active sequences and dynamically groups those with identical lengths, eliminating realignment for homogeneous groups. This strategy preserves the scaling efficiency of standard batching—where GPU parallelism drives throughput—while retaining the per-sequence acceleration benefits of speculation. At batch size 8, we achieve a 3× throughput improvement over batch size 1. Nevertheless, beyond batch size 8, throughput degrades as grouping success rates decline, forcing more frequent fallbacks to expensive realignment. Section 4 examines these scaling dynamics and the relationship between sequence diversity, grouping effectiveness, and alignment overhead.

082  
083  
084  
085  
086  
087  
Our experiments on SpecBench (Xia et al., 2024) yield two main results. First, **Correctness**: unlike prior approaches such as BSP and DSD, which suffer severe output corruption, our method preserves approximately 95% output equivalence across Vicuna-7B/68M (Zheng et al., 2023), Qwen3-8B/0.6B (Yang et al., 2025), and GLM-4-9B/0.6B (GLM et al., 2024) model pairs. Second, **Scalability**: at batch size 8, EXSPEC achieves up to a 3× speedup over batch size 1. Our contributions are summarized as follows:

- 089  
090  
091  
• We provide a correctness-first analysis of the ragged-tensor problem in batch speculative decoding, identifying precise synchronization requirements for correctness and explaining why existing methods fail (Section 2).
- 092  
093  
094  
• We present a unified solution that maintains correctness through precise synchronization invariants while avoiding their overhead via cross-batch scheduling of same-length sequence groups (Section 3).
- 095  
096  
097  
098  
• We experimentally demonstrate that our approach achieves both >95% output correctness and positive scaling through batch size 8, successfully multiplying batch parallelism with per-sequence speculation gains, whereas production systems (vLLM, SGLang) exhibit negative speedups (Section 4).

## 100 2 DESIGN SPACE ANALYSIS

101  
102  
103  
104  
105  
106  
107  
When sequences within a batch accept different numbers of draft tokens during verification, tensors become irregular, violating GPUs’ requirement for rectangular layouts—this is the ragged-tensor problem illustrated in Figure 2. Despite batching’s centrality to production deployments, existing implementations lack a principled design that preserves output equivalence with standard decoding while scaling with batch size. We identify three approaches to handle raggedness: *Masking*, *Rollback*, and *Dynamic Padding*. Yet, as our systematic analysis shows, current instantiations of these approaches fail to simultaneously maintain correctness and performance at scale. To close this

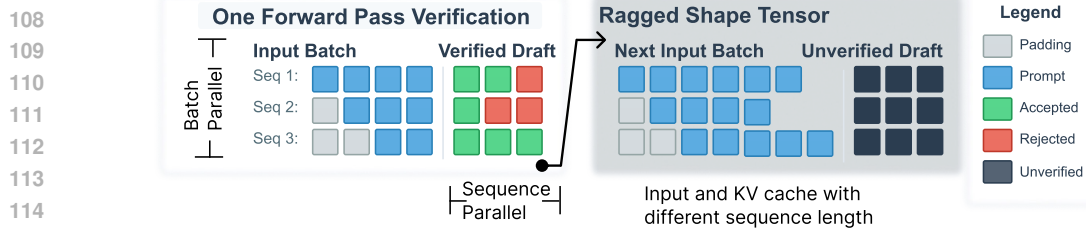


Figure 2: The ragged tensor problem in batch speculative decoding. Differing numbers of accepted draft tokens across sequences in the same batch lead to ragged-shaped input IDs tensors and KV Cache that disrupt subsequent batch operations.

---

**Algorithm 1** BatchVerify: Single Forward Pass
 

---

**Require:** Target model  $\mathcal{M}_t$ , Sequences  $\mathcal{S}$ , Draft tokens  $D$ , KV cache  
**Ensure:** Accepted tokens  $A$ , Bonus tokens  $B$

- 1: **if** first iteration **then**
- 2:    $\mathcal{X} \leftarrow \mathcal{S} \oplus D$
- 3: **else**
- 4:    $\mathcal{X} \leftarrow D$
- 5:    $\text{logits}, \text{KVCache} \leftarrow \mathcal{M}_t(\mathcal{X}, \text{KVCache})$
- 6:    $\text{pred\_tokens} \leftarrow \arg \max(\text{logits}, \text{dim}=\text{vocab})$
- 7:     **Vectorized first mismatch detection**
- 8:    $\text{matches} \leftarrow (\text{pred\_tokens} = D)$
- 9:    $J \leftarrow \arg \max(\neg \text{matches}, \text{dim}=\text{seq})$
- 10:   **Ragged shape acceptance, no vectorization**
- 11:   **for** each sequence  $i$  in batch **do**
- 12:      $A[i] \leftarrow D[i][:j]$
- 13:     **Get bonus token from first mismatch**
- 14:      $\text{bonus\_logit} \leftarrow \text{logits}[i, |\mathcal{S}[i]| + j]$
- 15:      $B[i] \leftarrow \arg \max(\text{bonus\_logit})$
- 16:   **return**  $A, B, \text{KVCache}$

---

**Algorithm 2** EQSPEC
 

---

**Require:** Draft model  $\mathcal{M}_d$ , Target model  $\mathcal{M}_t$ , Prompts  $\mathcal{P}$ , Max tokens  $T$ , Draft length  $K$   
**Ensure:** Generated sequences  $\mathcal{S}$

- 1:  $\mathcal{S} \leftarrow \text{Tokenize}(\mathcal{P})$  ▷ Batch left padding
- 2:  $\text{KVCache} \leftarrow \emptyset$
- 3: **while** until max new tokens **do**
- 4:   **Phase 1: Draft Generation**
- 5:     $D \leftarrow \mathcal{M}_d.\text{Generate}(\mathcal{S}, K)$
- 6:   **Phase 2: Batch Verification**
- 7:     $A, B, \text{KVCache} \leftarrow \text{BatchVerify}(\mathcal{M}_t, \mathcal{S}, D, \text{KVCache})$
- 8:     **See Figure 3 for illustration on index offset.**
- 9:   **Phase 3: Unpad-Append-Repad**
- 10:    **for** each sequence  $i$  in batch **do**
- 11:      $\mathcal{S}[i] \leftarrow \text{Unpad}(\mathcal{S}[i])$
- 12:      $\mathcal{S}[i] \leftarrow \mathcal{S}[i] \oplus A[i] \oplus B[i]$
- 13:      $\mathcal{S}, \text{offset} \leftarrow \text{BatchRepad}(\mathcal{S})$
- 14:     $\text{KVCache} \leftarrow \text{Realign}(\text{KVCache}, \text{offset})$
- 15: **return**  $\mathcal{S}$

---

gap, we first analyze the pitfalls of each approach and then introduce a correctness-first algorithmic design with explicit synchronization requirements for reliable batch speculative decoding.

**✗ Masking Approach (non-contiguous position IDs).** This approach operates directly on ragged tensors by masking rejected tokens in attention and reassigning position IDs so new tokens align with their content positions. Across verification rounds with varying rejections, sequences accumulate padding in various positions (middle and right), forming non-contiguous position IDs that standard Transformer implementations handle poorly. BSP (Su et al., 2023) attempts this via masking but fails to maintain position-ID consistency across iterations, yielding corrupted outputs (Figure 1). EAGLE’s experimental batching code<sup>1</sup> (Li et al., 2025) encounters similar framework limitations. Supporting non-contiguous position IDs would require custom CUDA kernels for each base model (Qian et al., 2024)—a prohibitive engineering cost that sacrifices portability.

**✗ Rollback Approach (speculation waste).** After each verification step, all sequences are truncated to the batch’s minimum accepted length (Wolf et al., 2020; kamilakesbi, 2024). This guarantees alignment but discards correctly verified tokens from faster sequences. As batch size grows and acceptance-rate variance widens, the waste compounds; in the extreme, one persistently rejecting sequence forces single-token progress for the entire batch. In effect, throughput collapses to that of the worst-performing sequence, undermining speculative gains and rendering the approach impractical at larger scales.

<sup>1</sup>While EAGLE’s main contribution concerns improved draft models rather than batching, its repository includes experimental batch-related code we analyzed for implementation challenges. <https://github.com/SafeAILab/EAGLE/issues/250>

✓ **Dynamic Padding Approach.** This approach realigns sequences after each verification by adjusting left padding to maintain right alignment, preserving all accepted tokens. While conceptually simple, correctness requires tight synchronization of position IDs, attention masks, and the KV-cache. DSD’s experimental code (Yan et al., 2025) follows this idea but merely repads at each step—adding varying left padding without ever unpadding—thereby inflating sequences. It also contains three critical errors: (i) sampling bonus tokens from the draft model rather than the target model; (ii) redundantly regenerating KV-cache entries, causing memory bloat; and (iii) desynchronizing padding, position IDs, and the KV-cache across iterations. Despite the overhead of repeated realignment, a correct dynamic-padding implementation fits within standard frameworks and preserves all verified tokens.

172 Among the three approaches, only dynamic padding is viable: position-ID schemes require custom  
173 kernels that undermine portability, and rollback discards verified tokens at rates that grow with batch  
174 size; dynamic padding maintains correctness within standard frameworks.

**Correctness Criterion.** We formalize the correctness requirement for batch speculative decoding. Under greedy decoding (temperature = 0), speculative decoding must yield outputs identical to standard autoregressive generation, and any token-level divergence indicates an implementation error. For temperature > 0, where outputs are sampled stochastically, speculative decoding must preserve the output distribution of the target model; that is, the probability of generating any token sequence must remain unchanged. This *losslessness*, whether measured by exact output equivalence or distributional equivalence, is the defining criterion of correct speculative decoding and the hallmark of an authentic implementation. Methods that achieve high throughput while violating this criterion, as we demonstrate for BSP and DSD in Figure 1, do not constitute valid speculative decoding regardless of their reported performance metrics.

## NEW

### 3 METHOD

188 We present a synchronization-aware approach to batch speculative decoding that co-designs cor-  
 189 rectness and efficiency. The core tension is that preserving correctness requires synchronizing pos-  
 190 ition IDs, attention masks, and the KV-cache across ragged tensors—an overhead that can consume  
 191 40% of computation. We introduce two complementary mechanisms: EQSPEC specifies and en-  
 192 forces the minimal synchronization invariants required for valid computation (Section 3.1), while  
 193 EXSPEC groups same-length sequences to avoid synchronization overhead (Section 3.3). Together,  
 194 these form a unified system in which correctness constraints drive scheduling, enabling both output  
 195 equivalence and practical performance.

### 3.1 MINIMAL BATCH REALIGNMENT: EqSPEC

199 Figure 3 illustrates the core challenge and our rem-  
 200 edy for maintaining correctness in batch speculative  
 201 decoding. After each verification round, sequences  
 202 accept different numbers of draft tokens, producing  
 203 ragged tensors that GPUs cannot process. To restore  
 204 a valid batch, we apply an *unpad-append-repad*  
 205 procedure that converts ragged outputs back to a  
 206 rectangular layout while preserving three invariants:  
 207 contiguous position IDs, valid attention masks, and  
 aligned KV-cache entries.

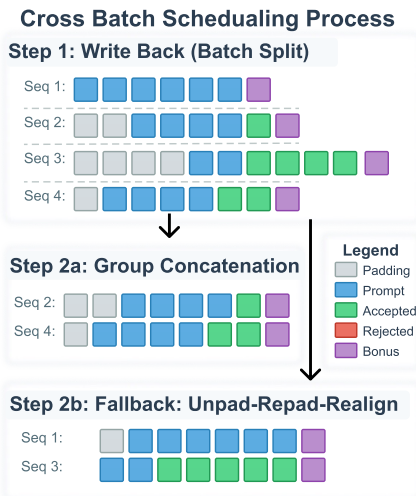
Correct implementation requires padding-agnostic position IDs that reset to zero at the first content token, attention masks that exclude padding tokens, and precise KV-cache realignment after each verification step (Algorithm 1). After *unpad-append-repad*, index offsets shift across sequences; consequently, position IDs and attention masks must be recomputed to preserve correct token relationships. Moreover, the bonus token introduces



Figure 3: EQSPEC synchronizes via unpad–append–repad.

216 a special case: it is sampled from the target model’s  
 217 output distribution at the first mismatch position after the verification forward pass has already completed.  
 218 Consequently, while it encodes the target’s authoritative correction, it lacks KV-cache entries in either the draft or target model because KV-cache is computed only for tokens that were present in the input sequence during the forward pass—and the bonus token, being an output, was not yet part of that input sequence. Therefore, it must be included in the next forward pass to create its KV-cache entries, further complicating synchronization. Finally, the realignment is resource-intensive: the KV-cache consists of rank-4 tensors (batch  $\times$  heads  $\times$  sequence  $\times$  dimension), and each padding adjustment triggers allocation and concatenation of high-dimensional zeros. Algorithm 2 details the complete EQSPEC procedure.  
 225

## 226 227 3.2 THEORETICAL SPEEDUP ANALYSIS



245 Figure 4: EXSPEC pools ragged sequences  
 246 by length, avoiding realignment; only un-  
 247 matched sequences need syncing, turning  
 248 fixed overhead into optional cost.

250 single-sequence analysis.

252 Two observations follow. First, when sequences within a batch share the same length, batch realign-  
 253 ment overhead is negligible; likewise, with very small draft models or prompt lookahead decoding  
 254 (Fu et al., 2024b),  $c_{\text{draft}}$  becomes small relative to verification. Second, and critically,  $c_{\text{overhead}}(B)$   
 255 scales superlinearly with batch size  $B$  due to the ragged-tensor problem (Section 4.3). This overhead  
 256 decomposes as  $c_{\text{overhead}}(B) = c_{\text{pad}}(B) + c_{\text{kv}}(B)$ , where  $c_{\text{pad}}(B)$  accounts for unpad–append–repad  
 257 operations and  $c_{\text{kv}}(B)$  for KV-cache realignment on rank-4 tensors. While  $c_{\text{draft}}$  and  $c_{\text{verify}}$  benefit  
 258 from GPU parallelism and remain relatively stable within the hardware’s batch-parallel regime, the  
 259 alignment overhead grows with both batch size and variance in acceptance rates across sequences.

## 260 261 3.3 CROSS-BATCH SCHEDULING: EXSPEC

262 Profiling EQSPEC shows that alignment overhead consumes 39.4% of computation at batch size 8,  
 263 rising to 46.7% at batch size 16. Because this cost is inherent to synchronizing ragged tensors, micro-  
 264 optimizing the primitives yields limited gains. Instead of accelerating these operations, EXSPEC  
 265 avoids them by scheduling.

266 EXSPEC differs from EQSPEC in how it manages sequence lifecycles. Rather than maintaining fixed  
 267 batches that require realignment after every verification, we introduce a *SequencePool* that holds  
 268 sequences individually in their ragged states. This enables three optimizations: (i) sequences that  
 269 complete (reach EOS) are immediately removed, avoiding wasted computation on finished items; (ii)  
*lazy realignment* defers synchronization until strictly necessary, keeping sequences in their natural

FIX

The speedup of speculative decoding depends on both the token-acceptance rate and computational costs. The original formulation by Leviathan et al. (2023) analyzes single-sequence performance, modeling the expected tokens generated per iteration as  $(1 - \alpha^{k+1})/(1 - \alpha)$ , where  $\alpha$  is the token acceptance rate (TAR) and  $k$  is the number of draft tokens per speculation round. This single-sequence view assumes negligible batch overhead and focuses purely on acceptance dynamics.

Batch speculative decoding, however, introduces additional complexities not captured by that model—most notably alignment overhead, which can dominate and degrade performance. We therefore introduce a batch-aware speedup model:

$$S = \frac{\alpha \cdot k}{c_{\text{draft}} + c_{\text{verify}} + c_{\text{overhead}}(B)} \quad (1)$$

where  $S$  denotes speedup relative to non-speculative decoding (i.e., running the target model alone),  $c_{\text{draft}}$  and  $c_{\text{verify}}$  are the relative costs of draft generation and target verification, and  $c_{\text{overhead}}(B)$  captures batch-dependent alignment overhead absent from

ragged form between steps; and (iii) *dynamic batch formation* over a sliding window of  $W > B$  sequences greatly increases the chance of finding same-length groups that can be concatenated without any realignment.

Figure 4 illustrates the flow. After verification, ragged sequences return directly to the pool without realignment. The scheduler then scans the active window and attempts to form batches of identical length. Same-length sequences concatenate directly—no padding adjustments, no position-ID recomputation, no KV-cache realignment—bypassing  $c_{\text{overhead}}(B)$ . Only when same-length grouping fails do we fall back to the expensive *unpad-append-repad* procedure from EQSPEC. Algorithm 3 formalizes this in four phases: dynamic batch formation (prioritizing same-length groups), draft generation, verification, and pool write-back with continuous window refresh. Combined with prompt-length sorting, grouping rates approach unity for similar workloads, turning the worst case (constant realignment) into the rare case.

## 4 EXPERIMENTS

We evaluate EQSPEC and EXSPEC along two dimensions often conflated in prior work: **correctness** (whether outputs match non-speculative generation) and **throughput** (tokens per second). Through systematic evaluation across three model families and comparisons with both research prototypes and production systems, we show that our approach uniquely preserves output equivalence while achieving competitive speedups.

## 4.1 EXPERIMENTAL SETUP

**Models.** To demonstrate generality, we evaluate three target–draft pairs: Vicuna-7B/68M (Zheng et al., 2023), Qwen3-8B/0.6B (Yang et al., 2025), and GLM-4-9B/0.6B (GLM et al., 2024). Unless otherwise noted, experiments use NVIDIA A100 80GB GPUs, PyTorch 2.7, HuggingFace Transformers 4.51.3, five draft tokens per speculation round, and greedy decoding for determinism.

**Evaluation and Datasets.** We use SpecBench (Xia et al., 2024), focusing on the first turn of each conversation because our evaluation targets offline batch inference rather than multi-turn interaction. We also use Multi30k (Elliott et al., 2016) for a controlled EXSPEC study that contrasts random sampling with an identical-length subset, isolating sequence-length diversity as the driver of grouping rate. For the main evaluation, we measure: (1) *Throughput*: tokens/s across batch sizes; and (2) *Correctness*: exact-match rate (full-sequence equivalence with non-speculative decoding) and partial-match rate (fraction of tokens matching until the first divergence). The partial-match metric helps localize failure modes—early divergence typically indicates position-ID or KV-cache misalignment.

**Batch Speculative Decoding Compared.** Following our design-space taxonomy (Section 2), we evaluate: (1) *Masking approaches*: **BSP** (Su et al., 2023) attempts masking with adaptive speculation but suffers position-ID inconsistencies (**BASS** (Qian et al., 2024) also follows this approach but requires custom CUDA kernels, limiting generality); (2) *Dynamic-padding approaches*: **DSD** (Yan et al., 2025) explores padding but mishandles the KV-cache, while **EQSPEC** implements correct synchronization and **EXSPEC** adds cross-batch scheduling; (3) *Reference baselines*: **Spec-1** (batch-size-1 speculation from Hugging Face Transformers), which does not support batch speculative

**Algorithm 3** EXSPEC: Cross-Batch Scheduling

```

Require: Draft and Target model  $\mathcal{M}_d, \mathcal{M}_t$ , Prompts  $\mathcal{P}$ , Window size  $W$ , Batch size  $B$ 
Ensure: Generated sequences  $S$ 
1:  $Pool \leftarrow \text{InitSequencePool}(\mathcal{P})$ 
2:  $\triangleright \text{Tokenize and optionally sort by length}$ 
3:  $Window \leftarrow \text{RefillWindow}(Pool, W)$ 
4: while  $Pool.\text{hasActive}()$  do
5:   Phase 1: Lazy Realignment
6:    $\mathcal{B}, mask, KV \leftarrow \text{GetBatch}(Window, B)$ 
7:    $\triangleright \text{Try same-length concatenation}$ 
8:    $\triangleright \text{Fallback to Unpad-Repad Realignment}$ 
9:   Phase 2: Draft Generation
10:   $D \leftarrow \mathcal{M}_d.\text{Generate}(\mathcal{B}, mask, K)$ 
11:  Phase 3: Batch Verification
12:   $A, B, KV \leftarrow \text{BatchVerify}(\mathcal{M}_t, \mathcal{B}, D, KV)$ 
13:  Phase 4: Write-Back and Window Refill
14:  for  $i \in \mathcal{B}$  do
15:     $Pool[i] \leftarrow Pool[i] \oplus A[i] \oplus B[i]$ 
16:     $Pool.KV[i] \leftarrow KV[i]$ 
17:    if  $\text{isComplete}(Pool[i])$  then
18:       $Pool.\text{deactivate}(i)$ 
19:     $Window \leftarrow \text{RefillWindow}(Pool, W)$ 
20:  return  $Pool.sequences$ 

```

Method	Vicuna		Qwen3		GLM4	
	Batch 1	Batch 4	Batch 1	Batch 4	Batch 1	Batch 4
<i>Batch-based Methods (vs. batch=1 non-spec)</i>						
Non-Spec-Batch	–	–	53.8	98.2	–	–
Spec-1	97.1	98.4	–	–	94.6	97.2
EQSPEC	97.3	98.6	92.1	98.6	94.6	96.9
EXSPEC	97.3	98.6	90.8	97.6	94.6	96.9
DSD	0.0	8.1	0.0	2.2	0.2	2.2
BSP	1.9	39.7	0.2	31.3	3.5	19.9
<i>Continuous Batching Systems (vs. own non-spec)</i>						
vLLM + Spec	96.9 / 98.0		65.6 / 78.5		72.7 / 84.5	
SGLang + EAGLE	69.8 / 79.5		47.7 / 65.4		–	
SGLang + EAGLE + Det	85.0 / 90.0		50.6 / 69.5		–	

Table 1: Correctness check reports exact match (E) and partial match (P) scores. Top: compares with batch=1 non-spec baseline. Bottom: with each system’s non-speculative mode (scores reported as E / P). Our approach sustains > 95% accuracy, while prior work (DSD, BSP) suffers major drops from KV-cache and position ID errors.

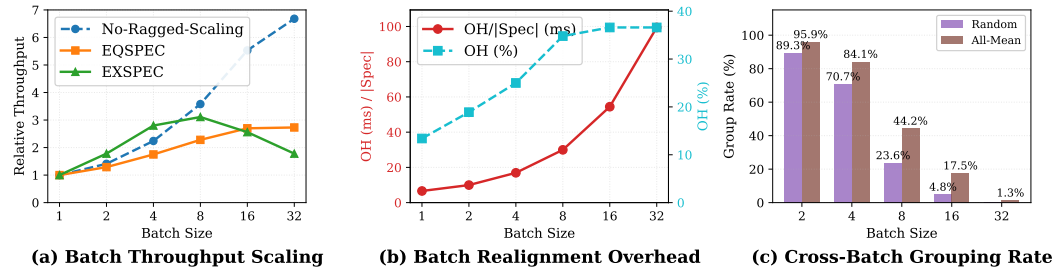


Figure 5: Decomposing batch speculative decoding performance. (a) Batch scaling efficiency: each method’s throughput normalized to its own BS=1 baseline, isolating scaling behavior from absolute performance. The No-Ragged-Scaling line shows measured autoregressive decoding throughput (not a theoretical bound), serving as a reference for how standard batching scales without ragged tensor overhead. (b) Alignment overhead grows super-linearly with batch size, consuming up to 38% of inference time, validating that  $c_{\text{overhead}}(B)$  dominates at scale. (c) Cross-batch grouping rates on Multi30k for random vs. uniform-length sequences, showing that length homogeneity transforms grouping effectiveness.

decoding<sup>2</sup>. We also compare with production systems **vLLM**<sup>3</sup> (Kwon et al., 2023) (which subsumes TETRIS (Wu et al., 2025) and TurboSpec (Liu et al., 2025) as vLLM forks) and **SGLang-EAGLE**<sup>4</sup> (Zheng et al., 2024; Li et al., 2024b; 2025), noting that their continuous batching and memory-management designs complicate direct comparison. We further test **SGLang-EAGLE-Deterministic** (SGLang Team, 2025), which enables deterministic execution to reduce numerical variance. No existing implementation uses rollback due to its inherent wastefulness.

## 4.2 OUTPUT CORRECTNESS VERIFICATION

We verify correctness using deterministic greedy decoding to eliminate sampling variance and enable precise bug isolation. This avoids metrics such as ROUGE (Qian et al., 2024), which can mask implementation failures (e.g., repetitive corruption can still score reasonably). Instead, we use exact match (any divergence) and partial match (fraction of tokens before the first mismatch) to diagnose failure modes.

<sup>2</sup><https://github.com/huggingface/transformers/issues/32165>

<sup>3</sup>We use the vLLM v0 engine because v1 deprecates speculative decoding.

<sup>4</sup>SGLang is compatible only with the EAGLE family; we compare Vicuna-7B/EAGLE2 and Qwen3-8B/EAGLE3. There are no available weights for GLM-4.

378 Table 1 reveals distinct patterns. Our methods maintain  $\approx 95\%$  exact match across settings, the re-  
 379 maining  $\approx 5\%$  divergence stems from numerical non-determinism in floating-point operations (He  
 380 & Lab, 2025) and tie-breaking in argmax sampling rather than algorithmic errors. By contrast  
 381 DSD and BSP fail catastrophically with different signatures. DSD’s near-zero scores indicate im-  
 382 mediate position-ID misalignment—the model fails from the first token. BSP shows higher par-  
 383 tial match (up to 39.7%) but low exact match, indicating gradual degradation: outputs are initially  
 384 correct before KV-cache drift misdirects attention, triggering repetition. These complementary pat-  
 385 terns—immediate failure vs. gradual decay—show how partial-match metrics reveal not just *that*  
 386 implementations fail, but *when* and *why*.

387 Production systems (vLLM, SGLang) introduce additional complexity. While both are accurate on  
 388 Vicuna, they degrade markedly on Qwen3. SGLang-EAGLE-Deterministic helps disambiguate the  
 389 cause: improved accuracy suggests most divergences stem from floating-point non-determinism (He  
 390 & Lab, 2025) rather than algorithmic bugs. Despite this, we show below that their throughput still  
 391 falls below non-speculative baselines.

392

### 393 4.3 OVERHEAD AND SCALING DYNAMICS

394

395 We now validate our theoretical predictions through five studies that decompose batch speculative  
 396 decoding performance. These experiments isolate alignment overhead growth, quantify its impact on  
 397 batch scaling, identify sequence diversity as the key bottleneck to grouping effectiveness, compare  
 398 against production systems, and provide mechanistic insights through overhead profiling.

399

400 **Batch scaling efficiency.** Figure 1 shows that EXSPEC outperforms EQSPEC in absolute through-  
 401 put by combining speculative and batching gains, yet EQSPEC exhibits negative scaling beyond  
 402 BS=8. To test whether batch speculative decoding can retain GPU-parallelism benefits despite  
 403 raggedness, Figure 5(a) measures *batch scaling efficiency*: each method’s throughput at batch size  
 404  $N$  divided by its own throughput at batch size 1. This normalization isolates how well each method  
 405 scales with batch size, independent of absolute performance differences. The *No-Ragged-Scaling*  
 406 line represents actual measured autoregressive decoding throughput (without speculation), similarly  
 407 normalized to its own BS=1 baseline; it is not a theoretical upper bound but rather a reference show-  
 408 ing how standard batching scales when no ragged tensor synchronization is required. A notable  
 409 effect emerges: EXSPEC initially exceeds this reference line. This occurs because each method is  
 410 normalized independently, and speculation converts memory-bound token generation into compute-  
 411 bound verification, which benefits more from GPU parallelism. Although EXSPEC may have lower  
 412 absolute throughput than standard decoding at BS=1 due to draft model overhead, its relative scaling  
 413 from BS=1 to BS=8 can surpass that of non-speculative decoding. However, at larger batch sizes,  
 414 alignment overhead dominates and the advantage inverts, confirming that  $c_{\text{overhead}}(B)$  eventually  
 415 overwhelms parallelism gains. The key finding is that correct batch speculative decoding need not  
 416 sacrifice batch scaling efficiency, given that prior methods either produce incorrect outputs or fail to  
 417 scale.

FIX

418

419 **Alignment overhead growth.** Figure 5(b) quantifies realignment costs via two metrics: percent-  
 420 age of total time spent on alignment (OH%) and per-round alignment time (OH/|Spec|). Over-  
 421 head rises from  $\sim 13\%$  at BS=1 to nearly 40% at BS=32, with per-round costs increasing even  
 422 more. This matches our prediction that  $c_{\text{pad}}(B) + c_{\text{kv}}(B)$  grows super-linearly with  $B$ . Crucially,  
 423 this is not merely an implementation inefficiency: the very operations required for correctness (un-  
 424 pad-append-repad and KV-cache realignment) become increasingly expensive as sequence lengths  
 425 diverge.

426

427 **Grouping rate  $\times$  sequence-length distribution.** Figure 5(c) probes whether cross-batch schedul-  
 428 ing limits are algorithmic or circumstantial via Multi30k. Comparing random sampling to an All-  
 429 Mean subset with identical lengths isolates the bottleneck: sequence diversity, not the method. Ran-  
 430 dom sampling shows grouping rates collapsing with batch size, whereas the All-Mean configuration  
 431 maintains high grouping effectiveness even at moderate scales, substantially reducing  $c_{\text{overhead}}(B)$ .  
 This contrast suggests that preprocessing strategies (e.g., bucketing, dynamic sorting) can push real  
 workloads toward the ideal, revealing untapped potential when scheduling is paired with workload  
 shaping.

Method	TPS	Spec	Time/Verif. (ms)	Verif. %	Draft %	Overhead %
EQSPEC	95.6	1469	24.88	44.9	27.4	27.7
EXSPEC	156.4	952	29.13	55.9	29.5	14.6

Table 2: Overhead anatomy of batch speculation methods. Despite slower per-verification time, EXSPEC achieves higher throughput by reducing total verification calls and minimizing alignment overhead through intelligent scheduling.

Batch Size	Method	Throughput	P50	P90	P99
1	EQSPEC	15.20	6.70	12.96	16.53
	EXSPEC	15.78	6.08	8.32	9.42
2	EQSPEC	26.70	7.96	14.78	19.06
	EXSPEC	30.54	9.75	<b>114.89</b>	<b>134.03</b>
4	EQSPEC	46.11	9.46	16.23	19.13
	EXSPEC	52.44	8.01	<b>53.21</b>	<b>70.35</b>
8	EQSPEC	76.03	11.26	19.23	22.50
	EXSPEC	77.54	9.16	19.13	<b>33.93</b>

Table 3: Latency-throughput tradeoff under simulated online serving with heterogeneous request lengths. Throughput is in tokens/s. P50, P90, and P99 denote the 50th, 90th, and 99th percentiles of request completion latency, respectively. Bold values indicate significantly worse tail latencies for EXSPEC.

**Overhead Anatomy.** Table 2 shows that EXSPEC attains higher throughput via a deliberate trade-off. Cross-batch scheduling cuts total verification calls by one-third and halves alignment overhead by grouping same-length sequences. The trade-off is memory locality: dynamic batching scatters KV-cache entries, increasing per-verification latency. Despite slower individual operations, the reduction in operation count yields a 64% overall throughput gain. This balance between operation count and efficiency suggests future work on improving KV-cache locality within the cross-batch framework.

#### 4.4 LATENCY-THROUGHPUT TRADEOFF IN ONLINE SERVING

To evaluate performance under realistic online serving conditions, we conducted experiments simulating dynamic request arrivals using full multi-turn conversations from SpecBench. We shuffled conversation turns to maximize length diversity and inserted new turns into the next available batch, measuring both throughput (tokens/s) and request completion latency (s) at P50/P90/P99 percentiles. Table 3 compares EQSPEC against EXSPEC across batch sizes 1, 2, 4, and 8.

NEW

Both methods achieve positive speedups under heterogeneous multi-turn workloads, with EXSPEC obtaining 2–14% higher throughput than EQSPEC through cross-batch grouping of same-length sequences. However, EXSPEC suffers 1.5–7.7× worse P90/P99 latencies when requests are delayed to enable grouping, as early requests must wait for later ones with matching lengths. This latency penalty is particularly severe at smaller batch sizes where grouping success rates are low (23.6% at batch size 2, as shown in Figure 5 c), causing head-of-line blocking that inflates tail latencies to over 100 seconds. In contrast, EQSPEC maintains predictable tail latency with P99 under 23 seconds across all batch sizes, making it suitable for latency-sensitive online serving where service-level objectives must be met. These results demonstrate that the choice between EQSPEC and EXSPEC depends on deployment requirements: EQSPEC provides stable, predictable latency for interactive applications, while EXSPEC maximizes throughput for offline batch processing where individual request latency is less critical. By offering both algorithms with explicit correctness guarantees, our work enables practitioners to match their batch speculation strategy to their specific operational constraints.

NEW

486 **5 RELATED WORK**

488 **Speculative Decoding.** Speculative decoding accelerates LLM inference by verifying draft tokens  
 489 in parallel. Two verification paradigms dominate: *sequence verification*—as in SpecDec and follow-  
 490 ups (Xia et al., 2023; Santilli et al., 2023; Yang et al., 2023; Hooper et al., 2023; Zhang et al., 2023;  
 491 Fu et al., 2024a)—which preserves the target model’s output distribution; and *tree verification*—e.g.,  
 492 Medusa/EAGLE variants (Miao et al., 2024; Spector & Re, 2023; Sun et al., 2023; He et al., 2023;  
 493 Cai et al., 2024; Li et al., 2024a;b; 2025)—which explores multiple branches to raise acceptance  
 494 rates. Recent works parallelize multiple draft sequences per request (Stewart et al., 2024; Lee et al.,  
 495 2024) but still verify each request independently. Approximate schemes (Kim et al., 2023; Zhong  
 496 et al., 2025) trade exactness for speed; our work assumes lossless verification to detect implementa-  
 497 tion errors rather than approximation artifacts.

498 **Batch Speculative Decoding.** Extending speculative decoding to batch settings introduces the  
 499 ragged tensor problem: when sequences accept different numbers of draft tokens, the resulting  
 500 variable-length tensors break GPU-friendly rectangular operations (Qian et al., 2024). Existing ap-  
 501 proaches face fundamental limitations detailed in Section 2. Position ID/masking approaches like  
 502 BSP (Su et al., 2023) suffer from position ID inconsistencies across iterations. Dynamic padding  
 503 approaches reveal critical implementation errors: both DSD (Yan et al., 2025) and Meta’s recent  
 504 work (Tang et al., 2025) incorrectly sample bonus tokens from the draft model’s distribution rather  
 505 than the target model’s, violating the fundamental correctness guarantee of speculative decoding.  
 506 This error compounds with improper KV-cache handling, producing corrupted outputs—BSP gen-  
 507 erates repetitive tokens while DSD produces `<unk>` symbols. BASS (Qian et al., 2024) sidesteps  
 508 these issues through custom CUDA kernels but sacrifices portability. These failures demonstrate  
 509 that the ragged tensor problem extends beyond performance to correctness itself, motivating our  
 510 cross-batch scheduling approach that maintains correctness while achieving batch scaling without  
 511 custom kernels.

512 **Production Systems for Speculative Decoding.** Serving stacks integrate speculation atop general  
 513 batching (vLLM, SGLang/EAGLE, and forks such as TETRIS and TurboSpec (Kwon et al., 2023;  
 514 Zheng et al., 2024; Li et al., 2025; Wu et al., 2025; Liu et al., 2025)). In practice, variable draft  
 515 acceptance clashes with continuous batching and paged attention, and our measurements indicate  
 516 scaling limits (e.g., small single-sequence gains that reverse at higher concurrency); some engines  
 517 have since reduced or deprecated speculative-decoding support. We intentionally build our refer-  
 518 ence implementation from scratch, prioritizing correctness checks; compatibility with continuous  
 519 batching, paged attention, and prefill–decode separation is orthogonal and left as future work.

521 **6 CONCLUSION**

523 We presented a correctness-first approach to batch speculative decoding that resolves the fundamen-  
 524 tal tension between maintaining output equivalence and achieving practical speedups. By identifying  
 525 the precise synchronization invariants required for correctness, we explained why existing methods  
 526 fail and established the minimal requirements for valid computation. In particular, our EQSPEC im-  
 527 plementation enforces these invariants but reveals that realignment overhead consumes up to 40%  
 528 of computation. By contrast, EXSPEC overcomes this limitation via cross-batch scheduling that  
 529 dynamically groups same-length sequences to bypass realignment entirely. Moreover, experiments  
 530 across three model families show that our approach uniquely preserves >95% output equivalence  
 531 while achieving up to 3× throughput improvement at batch size 8, hereby validating that a careful co-  
 532 design of correctness constraints and scheduling can multiply batch parallelism with per-sequence  
 533 speculation gains. Our findings on ragged shape tensor synchronization overhead and cross-batch  
 534 scheduling may inform future designs for production systems, where integrating speculation with  
 535 continuous batching remains an open challenge.

540 REFERENCES  
541

542 Tianle Cai, Yuhong Li, Zhengyang Geng, Hongwu Peng, Jason D. Lee, Deming Chen, and Tri Dao.  
543 Medusa: Simple LLM inference acceleration framework with multiple decoding heads. *CoRR*,  
544 abs/2401.10774, 2024. doi: 10.48550/ARXIV.2401.10774. URL <https://doi.org/10.48550/arXiv.2401.10774>.  
545

546 Charlie Chen, Sebastian Borgeaud, Geoffrey Irving, Jean-Baptiste Lespiau, Laurent Sifre, and John  
547 Jumper. Accelerating large language model decoding with speculative sampling. *arXiv preprint*  
548 *arXiv:2302.01318*, 2023.  
549

550 Desmond Elliott, Stella Frank, Khalil Sima'an, and Lucia Specia. Multi30k: Multilingual english-  
551 german image descriptions. In *Proceedings of the 5th Workshop on Vision and Language*, pp.  
552 70–74. Association for Computational Linguistics, 2016. doi: 10.18653/v1/W16-3210. URL  
553 <http://www.aclweb.org/anthology/W16-3210>.  
554

555 Yichao Fu, Peter Bailis, Ion Stoica, and Hao Zhang. Break the sequential dependency of llm infer-  
556 ence using lookahead decoding, 2024a.  
557

558 Yichao Fu, Peter Bailis, Ion Stoica, and Hao Zhang. Break the sequential dependency of llm infer-  
559 ence using lookahead decoding. *arXiv preprint arXiv:2402.02057*, 2024b.  
560

561 Team GLM, Aohan Zeng, Bin Xu, Bowen Wang, Chenhui Zhang, Da Yin, Diego Rojas, Guanyu  
562 Feng, Hanlin Zhao, Hanyu Lai, Hao Yu, Hongning Wang, Jiadai Sun, Jiajie Zhang, Jiale Cheng,  
563 Jiayi Gui, Jie Tang, Jing Zhang, Juanzi Li, Lei Zhao, Lindong Wu, Lucen Zhong, Mingdao Liu,  
564 Minlie Huang, Peng Zhang, Qinkai Zheng, Rui Lu, Shuaiqi Duan, Shudan Zhang, Shulin Cao,  
565 Shuxun Yang, Weng Lam Tam, Wenyi Zhao, Xiao Liu, Xiao Xia, Xiaohan Zhang, Xiaotao Gu,  
566 Xin Lv, Xinghan Liu, Xinyi Liu, Xinyue Yang, Xixuan Song, Xunkai Zhang, Yifan An, Yifan  
567 Xu, Yilin Niu, Yuantao Yang, Yueyan Li, Yushi Bai, Yuxiao Dong, Zehan Qi, Zhaoyu Wang,  
568 Zhen Yang, Zhengxiao Du, Zhenyu Hou, and Zihan Wang. Chatglm: A family of large language  
569 models from glm-130b to glm-4 all tools, 2024.  
570

571 Horace He and Thinking Machines Lab. Defeating nondeterminism in llm infer-  
572 ence. *Thinking Machines Lab: Connectionism*, 2025. doi: 10.64434/tm1.20250910.  
573 <https://thinkingmachines.ai/blog/defeating-nondeterminism-in-llm-inference/>.  
574

575 Zhenyu He, Zexuan Zhong, Tianle Cai, Jason D. Lee, and Di He. REST: retrieval-based speculative  
576 decoding. *CoRR*, abs/2311.08252, 2023. doi: 10.48550/ARXIV.2311.08252. URL <https://doi.org/10.48550/arXiv.2311.08252>.  
577

578 Coleman Hooper, Sehoon Kim, Hiva Mohammadzadeh, Hasan Genc, Kurt Keutzer, Amir Gholami,  
579 and Yakun Sophia Shao. SPEED: speculative pipelined execution for efficient decoding. *CoRR*,  
abs/2310.12072, 2023. doi: 10.48550/ARXIV.2310.12072. URL <https://doi.org/10.48550/arXiv.2310.12072>.  
580

581 kamilakesbi. Enable speculative decoding with batch size  $\zeta$  1 (github issue #32165). <https://github.com/huggingface/transformers/issues/32165>, 2024. Hugging Face *transformers*.  
582 Opened 2024-07-23. Accessed 2025-09-24.  
583

584 Sehoon Kim, Karttikeya Mangalam, Suhong Moon, Jitendra Malik, Michael W. Mahoney,  
585 Amir Gholami, and Kurt Keutzer. Speculative decoding with big little decoder. In Alice Oh,  
586 Tristan Naumann, Amir Globerson, Kate Saenko, Moritz Hardt, and Sergey Levine  
587 (eds.), *Advances in Neural Information Processing Systems 36: Annual Conference on Neu-  
588 ral Information Processing Systems 2023, NeurIPS 2023, New Orleans, LA, USA, Decem-  
589 ber 10 - 16, 2023*, 2023. URL [http://papers.nips.cc/paper\\_files/paper/2023/hash/7b97adeafa1c51cf65263459ca9d0d7c-Abstract-Conference.html](http://papers.nips.cc/paper_files/paper/2023/hash/7b97adeafa1c51cf65263459ca9d0d7c-Abstract-Conference.html).  
590

591 Woosuk Kwon, Zhuohan Li, Siyuan Zhuang, Ying Sheng, Lianmin Zheng, Cody Hao Yu, Joseph E.  
592 Gonzalez, Hao Zhang, and Ion Stoica. Efficient memory management for large language model  
593 serving with pagedattention. In *Proceedings of the ACM SIGOPS 29th Symposium on Operating  
Systems Principles*, 2023.

594 Minjae Lee, Wonjun Kang, Minghao Yan, Christian Classen, Hyung Il Koo, and Kangwook Lee.  
 595 In-batch ensemble drafting: Toward fast and robust speculative decoding for multimodal language  
 596 models, 2024. URL <https://openreview.net/forum?id=8o7131Lm83>.

597

598 Yaniv Leviathan, Matan Kalman, and Yossi Matias. Fast inference from transformers via speculative  
 599 decoding. In *International Conference on Machine Learning*, pp. 19274–19286. PMLR, 2023.

600

601 Yuhui Li, Fangyun Wei, Chao Zhang, and Hongyang Zhang. Eagle: Speculative sampling requires  
 602 rethinking feature uncertainty. In *International Conference on Machine Learning*, pp. 28935–  
 603 28948. PMLR, 2024a.

604

605 Yuhui Li, Fangyun Wei, Chao Zhang, and Hongyang Zhang. Eagle-2: Faster inference of language  
 606 models with dynamic draft trees. In *Proceedings of the 2024 Conference on Empirical Methods  
 607 in Natural Language Processing*, pp. 7421–7432, 2024b.

608

609 Yuhui Li, Fangyun Wei, Chao Zhang, and Hongyang Zhang. EAGLE-3: Scaling up inference  
 610 acceleration of large language models via training-time test, 2025. URL <https://arxiv.org/abs/2503.01840>.

611

612 Xiaoxuan Liu, Jongseok Park, Langxiang Hu, Woosuk Kwon, Zhuohan Li, Chen Zhang, Kuntai Du,  
 613 Xiangxi Mo, Kaichao You, Alvin Cheung, Zhijie Deng, Ion Stoica, and Hao Zhang. Turbospec:  
 614 Closed-loop speculation control system for optimizing llm serving goodput, 2025. URL <https://arxiv.org/abs/2406.14066>.

615

616 Xupeng Miao, Gabriele Oliaro, Zhihao Zhang, Xinhao Cheng, Zeyu Wang, Zhengxin Zhang, Rae  
 617 Ying Yee Wong, Alan Zhu, Lijie Yang, Xiaoxiang Shi, Chunan Shi, Zhuoming Chen, Daiyaan  
 618 Arfeen, Reyna Abhyankar, and Zhihao Jia. Specinfer: Accelerating large language model serv-  
 619 ing with tree-based speculative inference and verification. In *Proceedings of the 29th ACM  
 620 International Conference on Architectural Support for Programming Languages and Operat-  
 621 ing Systems, Volume 3*, ASPLOS '24, pp. 932–949, New York, NY, USA, 2024. Association  
 622 for Computing Machinery. ISBN 9798400703867. doi: 10.1145/3620666.3651335. URL  
 623 <https://doi.org/10.1145/3620666.3651335>.

624

625 Haifeng Qian, Sujan Kumar Gonugondla, Sungsoo Ha, Mingyue Shang, Sanjay Krishna Gouda,  
 626 Ramesh Nallapati, Sudipta Sengupta, Xiaofei Ma, and Anoop Deoras. Bass: Batched attention-  
 627 optimized speculative sampling. In *Findings of the Association for Computational Linguistics  
 628 ACL 2024*, pp. 8214–8224, 2024.

629

630 Andrea Santilli, Silvio Severino, Emilian Postolache, Valentino Maiorca, Michele Mancusi, Ric-  
 631 cardo Marin, and Emanuele Rodolà. Accelerating transformer inference for translation via  
 632 parallel decoding. In Anna Rogers, Jordan L. Boyd-Graber, and Naoaki Okazaki (eds.), *Pro-  
 633 ceedings of the 61st Annual Meeting of the Association for Computational Linguistics (Vol-  
 634 ume 1: Long Papers)*, ACL 2023, Toronto, Canada, July 9–14, 2023, pp. 12336–12355. As-  
 635 sociation for Computational Linguistics, 2023. doi: 10.18653/v1/2023.acl-long.689. URL  
 636 <https://doi.org/10.18653/v1/2023.acl-long.689>.

637

638 SGLang Team. Enabling deterministic inference for sglang. <https://lmsys.org/blog/2025-09-22-sqlang-deterministic/>, September 2025. LMSYS Org Blog, published Sep 22,  
 639 2025.

640

641 Benjamin Spector and Chris Re. Accelerating LLM inference with staged speculative decoding.  
 642 *CoRR*, abs/2308.04623, 2023. doi: 10.48550/arXiv.2308.04623. URL <https://doi.org/10.48550/arXiv.2308.04623>.

643

644 Lawrence Stewart, Matthew Trager, Sujan Kumar Gonugondla, and Stefano Soatto. The n-grammys:  
 645 Accelerating autoregressive inference with learning-free batched speculation. *arXiv preprint  
 646 arXiv:2411.03786*, 2024.

647

648 Qidong Su, Christina Giannoula, and Gennady Pekhimenko. The synergy of speculative decoding  
 649 and batching in serving large language models. *arXiv preprint arXiv:2310.18813*, 2023.

648 Ziteng Sun, Ananda Theertha Suresh, Jae Hun Ro, Ahmad Beirami, Himanshu Jain, and Fe-  
 649 lix X. Yu. Spectr: Fast speculative decoding via optimal transport. In Alice Oh, Tris-  
 650 tan Naumann, Amir Globerson, Kate Saenko, Moritz Hardt, and Sergey Levine (eds.), *Ad-*  
*651 vances in Neural Information Processing Systems 36: Annual Conference on Neural In-*  
*652 formation Processing Systems 2023, NeurIPS 2023, New Orleans, LA, USA, December*  
*653 10 - 16, 2023, 2023.* URL [http://papers.nips.cc/paper\\_files/paper/2023/hash/6034a661584af6c28fd97a6f23e56c0a-Abstract-Conference.html](http://papers.nips.cc/paper_files/paper/2023/hash/6034a661584af6c28fd97a6f23e56c0a-Abstract-Conference.html).

655 Bangsheng Tang, Carl Chengyan Fu, Fei Kou, Grigory Sizov, Haoci Zhang, Jason Park, Jiawen  
 656 Liu, Jie You, Qirui Yang, Sachin Mehta, et al. Efficient speculative decoding for llama at scale:  
 657 Challenges and solutions. *arXiv preprint arXiv:2508.08192*, 2025.

658 Thomas Wolf, Lysandre Debut, Victor Sanh, Julien Chaumond, Clement Delangue, Anthony Moi,  
 659 Pierrick Cistac, Tim Rault, Rémi Louf, Morgan Funtowicz, Joe Davison, Sam Shleifer, Patrick  
 660 von Platen, Clara Ma, Yacine Jernite, Julien Plu, Canwen Xu, Teven Le Scao, Sylvain Gugger,  
 661 Mariama Drame, Quentin Lhoest, and Alexander M. Rush. Transformers: State-of-the-art natural  
 662 language processing. In *Proceedings of the 2020 Conference on Empirical Methods in Natural*  
*663 Language Processing: System Demonstrations*, pp. 38–45, Online, October 2020. Association for  
 664 Computational Linguistics. URL <https://www.aclweb.org/anthology/2020.emnlp-demos.6>.

665 Zhaoxuan Wu, Zijian Zhou, Arun Verma, Alok Prakash, Daniela Rus, and Bryan Kian Hsiang Low.  
 666 Tetris: Optimal draft token selection for batch speculative decoding. In *Proceedings of the 63rd*  
*667 Annual Meeting of the Association for Computational Linguistics (ACL)*, 2025.

668 Heming Xia, Tao Ge, Peiyi Wang, Si-Qing Chen, Furu Wei, and Zhifang Sui. Speculative decod-  
 669 ing: Exploiting speculative execution for accelerating seq2seq generation. In Houda Bouamor,  
 670 Juan Pino, and Kalika Bali (eds.), *Findings of the Association for Computational Linguis-*  
*671 tics: EMNLP 2023, Singapore, December 6-10, 2023*, pp. 3909–3925. Association for Com-  
 672 putational Linguistics, 2023. doi: 10.18653/V1/2023.FINDINGS-EMNLP.257. URL <https://doi.org/10.18653/v1/2023.findings-emnlp.257>.

673 Heming Xia, Zhe Yang, Qingxiu Dong, Peiyi Wang, Yongqi Li, Tao Ge, Tianyu Liu, Wenjie Li, and  
 674 Zhifang Sui. Unlocking efficiency in large language model inference: A comprehensive survey  
 675 of speculative decoding. In Lun-Wei Ku, Andre Martins, and Vivek Srikumar (eds.), *Findings*  
*676 of the Association for Computational Linguistics ACL 2024*, pp. 7655–7671, Bangkok, Thailand  
 677 and virtual meeting, August 2024. Association for Computational Linguistics. doi: 10.18653/v1/2024.findings-acl.456. URL <https://aclanthology.org/2024.findings-acl.456>.

678 Minghao Yan, Saurabh Agarwal, and Shivaram Venkataraman. Decoding speculative decoding. In  
 679 *Proceedings of the 2025 Conference of the Nations of the Americas Chapter of the Association*  
*680 for Computational Linguistics: Human Language Technologies (Volume 1: Long Papers)*, pp.  
 681 6460–6473, 2025.

682 An Yang, Anfeng Li, Baosong Yang, Beichen Zhang, Binyuan Hui, Bo Zheng, Bowen Yu, Chang  
 683 Gao, Chengan Huang, Chenxu Lv, Chujie Zheng, Dayiheng Liu, Fan Zhou, Fei Huang, Feng Hu,  
 684 Hao Ge, Haoran Wei, Huan Lin, Jialong Tang, Jian Yang, Jianhong Tu, Jianwei Zhang, Jianxin  
 685 Yang, Jiaxi Yang, Jing Zhou, Jingren Zhou, Junyang Lin, Kai Dang, Keqin Bao, Kexin Yang,  
 686 Le Yu, Lianghao Deng, Mei Li, Mingfeng Xue, Mingze Li, Pei Zhang, Peng Wang, Qin Zhu, Rui  
 687 Men, Ruize Gao, Shixuan Liu, Shuang Luo, Tianhao Li, Tianyi Tang, Wenbiao Yin, Xingzhang  
 688 Ren, Xinyu Wang, Xinyu Zhang, Xuancheng Ren, Yang Fan, Yang Su, Yichang Zhang, Yinger  
 689 Zhang, Yu Wan, Yuqiong Liu, Zekun Wang, Zeyu Cui, Zhenru Zhang, Zhipeng Zhou, and Zihan  
 690 Qiu. Qwen3 technical report. *arXiv preprint arXiv:2505.09388*, 2025.

691 Seongjun Yang, Gibbeum Lee, Jaewoong Cho, Dimitris S. Papailiopoulos, and Kangwook Lee.  
 692 Predictive pipelined decoding: A compute-latency trade-off for exact LLM decoding. *CoRR*,  
 693 abs/2307.05908, 2023. doi: 10.48550/ARXIV.2307.05908. URL <https://doi.org/10.48550/arXiv.2307.05908>.

694 Jun Zhang, Jue Wang, Huan Li, Lidan Shou, Ke Chen, Gang Chen, and Sharad Mehrotra. Draft  
 695 & verify: Lossless large language model acceleration via self-speculative decoding. *CoRR*,

702       abs/2309.08168, 2023. doi: 10.48550/arXiv.2309.08168. URL <https://doi.org/10.48550/arXiv.2309.08168>.

703

704

705       Lianmin Zheng, Wei-Lin Chiang, Ying Sheng, Siyuan Zhuang, Zhanghao Wu, Yonghao Zhuang,  
706       Zi Lin, Zhuohan Li, Dacheng Li, Eric. P Xing, Hao Zhang, Joseph E. Gonzalez, and Ion Stoica.  
707       Judging Ilm-as-a-judge with mt-bench and chatbot arena, 2023.

708

709       Lianmin Zheng, Liangsheng Yin, Zhiqiang Xie, Chuyue Livia Sun, Jeff Huang, Cody Hao Yu, Shiyi  
710       Cao, Christos Kozyrakis, Ion Stoica, Joseph E Gonzalez, et al. Sglang: Efficient execution of  
711       structured language model programs. *Advances in neural information processing systems*, 37:  
712       62557–62583, 2024.

713       Meiyu Zhong, Noel Teku, and Ravi Tandon. Speeding up speculative decoding via sequential ap-  
714       proximate verification. *arXiv preprint arXiv:2502.04557*, 2025.

715

716

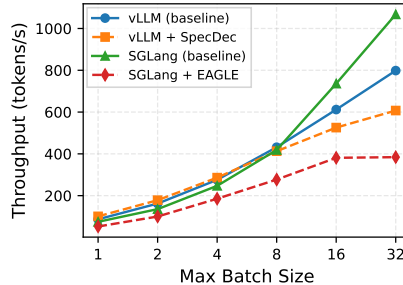
## A APPENDIX

### BATCH SCALING OF SPECULATIVE DECODING IN vLLM AND SGLANG

FIX

721       **Production systems limitation.** Figure 6 shows that production frameworks struggle with batch  
722       speculative decoding. Although our method is not directly comparable to continuous-batching sys-  
723       tems (which vary effective batch size dynamically), the trend is consistent: vLLM’s speculative  
724       decoding underperforms its baseline at high concurrency, and SGLang+EAGLE is slower than non-  
725       speculative generation across all batch sizes. vLLM’s v0 engine previously used batch expansion to  
726       sidestep the ragged tensor problem: instead of verifying draft tokens [1, 2, 3] together and handling  
727       variable acceptance lengths, it duplicated each sequence  $K$  times with variants [1], [1,2], [1,2,3],  
728       verified all variants in one pass, then kept only the longest correct prefix. This approach was dep-  
729       recated in v1 (vllm-project/vllm#17984) because it wastes  $K \times$  memory and  $K \times$  compute—if only  
730       token 1 is accepted, the longer variants consumed resources for nothing. This caused GPU memory  
731       overflow at scale and broke CUDA graph compatibility.

FIX



742       Figure 6: Speculative decoding lags non-speculative baselines, with larger batches further degrading  
743       throughput.

## DISCUSSION

NEW

748       Batch parallelism and per-sequence speculative decoding represent two orthogonal acceleration  
749       strategies that should, in principle, multiply together: batching exploits GPU parallelism across se-  
750       quences while speculation reduces sequential token dependencies within each sequence. However,  
751       when combining these techniques in practice, the ragged tensor problem emerges as a fundamental  
752       obstacle that breaks this multiplicative relationship. Different sequences accept different numbers  
753       of draft tokens, desynchronizing position IDs, attention masks, and KV-cache state across the batch.  
754       A correctly implemented batch speculative decoding, as we provide through EQSPEC and EXSPEC,  
755       preserves the multiplicative gains but incurs an inherent realignment cost that consumes up to 40%  
of computation. Critically, batch speculation amplifies per-sequence gains; it cannot create them.

756 If a draft-target pair shows no speedup at batch size 1 due to low acceptance rates or high draft  
 757 overhead, batching cannot recover what does not exist at the single-sequence level. Our work estab-  
 758 lishes the synchronization invariants required for correctness, quantifies their irreducible costs, and  
 759 demonstrates through cross-batch scheduling that intelligent system design can mitigate, though not  
 760 eliminate, the overhead of maintaining output equivalence at scale.

NEW

761

## 762 REPRODUCIBILITY STATEMENT

763

764 We provide our complete implementation in the Supplementary Material, including all hyperparam-  
 765 eters, experimental configurations, and model specifications detailed in Section 4. Our correctness  
 766 verification framework using exact and partial match metrics enables deterministic validation of both  
 767 our results and future implementations. All experiments use publicly available models and datasets  
 768 for reproducibility.

769

770 **Model Configurations.** We evaluate three target-draft model pairs: Vicuna-7B (lmsys/vicuna-7b-  
 771 v1.3) with a 68M draft model (double7/vicuna-68m), Qwen3-8B (Qwen/Qwen3-8B) with Qwen3-  
 772 0.6B (Qwen/Qwen3-0.6B), and GLM-4-9B (zai-org/GLM-4-9B-0414) with a 0.6B draft model  
 773 (jukofyork/GLM-4.5-DRAFT-0.6B-v3.0). All models were loaded in FP16 precision with greedy  
 774 decoding (temperature=0, top\_p=1.0) to ensure deterministic outputs. We use five draft tokens per  
 775 speculation round across all experiments unless otherwise specified.

776

777 **Production Systems Configuration.** We evaluated two production inference systems for compari-  
 778 son: vLLM version 0.9.1 and SGLang commit c4e314f (the deterministic decoding had not merged  
 779 to the stable version at the time of submission, so we compiled it from source). For vLLM, we  
 780 used the V0 engine with speculative decoding enabled, as the V1 engine does not support draft  
 781 model speculative decoding<sup>5</sup>. For SGLang, we used EAGLE-based speculation with model-specific  
 782 draft models: yuhuili/EAGLE-Vicuna-7B-v1.3 for Vicuna-7B and Tengyunw/qwen3\_8b\_eagle3 for  
 783 Qwen3-8B. GLM-4 was not evaluated with SGLang due to the unavailability of compatible EAGLE  
 784 draft models. We tested both standard SGLang inference and SGLang with deterministic mode en-  
 785 abled (SGLang Team, 2025) to isolate floating-point non-determinism from algorithmic correctness  
 786 issues.

787

## 788 DISCLOSE ON LLM USAGE

789

790 We used Large Language Models as assistive tools in preparing this manuscript: GPT-5 and Claude  
 791 Opus 4.1 for polishing writing (grammar correction and sentence restructuring), generating concep-  
 792 tual diagram illustrations, and writing unit tests; NVIDIA/Parakeet-TDT-0.6B-v3 for voice input  
 793 transcription. LLMs were not used for research ideation, experimental design, data analysis, or  
 794 scientific conclusions. All core algorithmic implementations and scientific contributions are solely  
 795 from the authors. We take full responsibility for all content in this paper.

796

## 797 ETHICS STATEMENT

798

799 This work focuses on improving the efficiency of LLM inference without altering model outputs or  
 800 introducing biases. Our correctness-preserving approach ensures that acceleration techniques do not  
 801 compromise model safety or reliability. Our open-source release enables reproducible research and  
 802 transparent evaluation of batch speculative decoding techniques.

803

804

805

806

807

808

809

<sup>5</sup><https://github.com/vllm-project/vllm/issues/21797>